MoST Research Project Proposal Form CM03 Energy Stable Time Discretizations for Fractional-in-space Allen-Cahn Equations. (2022/8/1-2023/7/31)

Wei-Cheng Wang
Department of Mathematics
National Tsing Hua University

1 Introduction

During the past few decades, scientists have been exploring fractional calculus as a tool for developing more sophisticated mathematical models that can accurately describe complex anomalous systems [36, 8, 32, 41]. Among different fractional operators, the fractional Laplacian has been intensively studied in the recent literature. It corresponds to one of the most important cases where the jump direction in the Lévy process is isotropic. The fractional Laplacian has been used in place of the integer-order Laplacian in many applications, including, for example, Fractional reaction-diffusion equations [45] Quasi-geostrophic equation [12] Porous medium equation [4, 35] The Schrodinger equation [24] and Ultrasound equation [40, 10]

In this MoST project, we will focus on the fractional-in-space Allen-Cahn equations (FiSAC):

$$\begin{aligned} &u_t + \mathcal{L}u + f(u) = 0 \quad \text{in } \Omega \\ &u = 0 \quad \text{on } \partial\Omega \end{aligned} \tag{1}$$

and aim to develop robust and efficient time discretization for (1). Here

$$f(u) = u^3 - u = F'(u), \qquad \text{where } F(u) = \frac{1}{4}(u^2-1)^2$$

and $\mathcal{L} = \epsilon^2(-\Delta)_{\mathrm{R}}^{\alpha/2}$ is the Riesz fractional Laplacian with $1 < \alpha < 2$ (see section 1.1 for definitions of various fractional Laplacians). Compared to standard Allen-Cahn equations, the fractional model (1) replaces the standard Laplacian by fractional derivative.

In recent years, there has been significant interest in using the diffusive-interface phase field approach for modeling the mesoscale morphological pattern formation and interface motion. One of the very effective mathematical models describing these physical phenomena is the Allen–Cahn equation introduced in 1979 [1]. Roughly speaking, the Allen-Cahn equations (1) describes regions with $u \approx 1$ and $u \approx -1$ grow and decay at the expense of one another [1]. It is noted that the FiSAC equation (1) has attracted many attentions in recent years. For example, Burrage et al. [7] proposed an implicit finite element scheme, Bueno-Orovio et al. [6] considered the Fourier spectral methods. In [18], the authors considered the Crank-Nicolson time discretization in 1D.

1.1 Definitions of fractional Laplacian in $\mathbf{R}^d$ and bounded domains

def

The fractional Laplacian in $\mathbf{R}^d$ can be defined in many equivalent ways. For example,

1. **Fractional Laplacian in $\mathbf{R}^d$ using Fourier representation**

$$\mathcal{F}((-\Delta^{\alpha/2}u))(\xi) = |\xi|^{\alpha}\mathcal{F}(u).$$

2. **Fractional Laplacian in $\mathbf{R}^d$ using integral representation**

$$(-\Delta)^{\alpha/2}u(x) = -c_{\alpha,d}\mathrm{PV}\int_{\mathbf{R}^d}\frac{u(x)-u(y)}{|x-y|^{d+\alpha}}dy$$

where

$$c_{\alpha,d} = \frac{2^{\alpha}\Gamma(\frac{d+\alpha}{2})}{\pi^{d/2}\left|\Gamma(-\frac{\alpha}{2})\right|}$$

A more comprehensive review of various definitions of the fractional Laplacian in $\mathbf{R}^d$ and their equivalence can be found in Kw17 [23].

However, when these definitions are restricted to bounded domains, the associated boundary conditions lead to distinct operators. Some of the mostly well known definitions include:

1. The **Integral (Dirichlet) fractional Laplacian on Ω.** The fractional Laplacian of $u(x)$, $x \in \Omega$ is defined through first extending $u(x)$ to a function in $\mathbf{R}^d$:

$$\tilde{u}(x) = \begin{cases} u(x), & x \in \Omega \\ 0, & x \in \Omega^c \end{cases}$$

and then the usual fractional Laplacian definition is used

$$(-\Delta)_{\mathrm{I}}^{\alpha/2}u(x) := (-\Delta)^{\alpha/2}\tilde{u}(x)$$

where the right hand side is defined through Fourier transform and its inverse

$$(-\Delta)^{\alpha/2}\tilde{u} := \mathcal{F}^{-1}(|\xi|^{\alpha}\mathcal{F}\tilde{u})$$

2. The **Spectral fractional Laplacian on Ω.**

The fractional operator is obtained via a spectral definition, that is

$$(-\Delta)_{\mathrm{S}}^{\alpha/2}u(x) := \sum_{i\in\mathbf{N}} u_i\lambda_i^{\alpha/2}\varphi_i(x) \quad (2)$$

SLap

where φ_i, $\lambda_i > 0$ are eigenfunctions and eigenvalues of the standard Laplacian in Ω with homogeneous Dirichlet boundary data,

$$\begin{cases} -\Delta\varphi_i = \lambda_i\varphi_i, & \text{in } \Omega \\ \varphi_i = 0, & \text{on } \partial\Omega \end{cases}$$

3. The **Regional (Riesz) fractional Laplacian on Ω.**

   This definition is carried out through restricting the integration domain to Ω.

$$(-\Delta)_{\mathrm{R}}^{\alpha/2} u(x) = -c_{\alpha,d}\mathrm{PV}\int_{\Omega} \frac{u(x)-u(y)}{|x-y|^{d+\alpha}}dy$$

   where

$$c_{\alpha,d} = \frac{2^{\alpha}\Gamma(\frac{d+\alpha}{2})}{\pi^{d/2}\left|\Gamma(-\frac{\alpha}{2})\right|}$$

Further results on stochastic interpretation and analytic properties of these fractional Laplacians can be found in [27].

In this MoST proposal, we consider fractional Laplacian on a bounded domain $\Omega \subset \mathbf{R}^d$ with zero Dirichlet boundary conditions (i.e. $u = 0$ on $\partial\Omega$). Both the Fourier and integral representation above can be naturally extended to bounded domains by extending $u = 0$ on $\mathbf{R}^d \setminus \Omega$ (and remain equivalent). In practice, the integral representation version is more convenient for numerical purpose on bounded domains and is the most widely used in the literature.

2 Project Description

The fractional Allen–Cahn equation (1) can be viewed an L^2-gradient flow of the following fractional analogue version of Ginzburg– Landau free energy functional

$$\mathcal{E}(u) = \int_{\Omega} F(u) + \frac{1}{2}u\mathcal{L}u \tag{3}$$

Similar to standard Allen-Cahn equations, the fractional model satisfies the energy decreasing property:

$$\frac{d}{dt}\mathcal{E}(u) = -\|u_t\|^2 \leq 0 \tag{4}$$

With regarding to this nonlinear energy stability, many numerical works have been devoted to the solutions of the (standard) Allen–Cahn equation, see, e.g., [11, 14, 15, 16, 17, 19, 20, 46, 47]. In the past few years, the numerical stability has been mostly restricted to this energy decreasing property. This is in particular becoming popular due to the convex concave splitting idea of Eyre [14], which turns out to be very effective for gradient flows but ends up with a nonlinear time stepping scheme.

To over come the difficulties associated with the nonlinear time stepping scheme, a conventional wisdom is to perform a suitable operator splitting

$$\mathcal{L}(u) = \mathcal{L}_0(u) + \big(\mathcal{L}(u) - \mathcal{L}_0(u)\big) \tag{5}$$

and treat $\mathcal{L}_0(u)$ and $\mathcal{L}(u) + f(u) - \mathcal{L}_0(u)$ separately. Typically, $\mathcal{L}_0$ is a dominant linear operator. To stabilize the time stepping, $\mathcal{L}_0(u)$ is discretized implicitly, while $\mathcal{L}(u) + f(u) -$

$\mathcal{L}_0(u)$ is discretized explicitly. so that the time marching is stable with fast direct solvers for the resulting linear system:

$$\frac{u^{n+1}-u^n}{\Delta t} + \mathcal{L}_0(u^{n+1}) = \mathcal{L}_0(u^n) - \mathcal{L}(u^n) - f(u^n), \tag{6}$$

For example, for standard Allen-Cahn equations, one could take $\mathcal{L}_0 u = -\epsilon^2 \Delta u + Su$ with $S > 0$ large enough to stabilize the nonlinear term $f(u)$. This results to the following linear system:

$$\frac{u^{n+1}-u^n}{\Delta t} + \mathcal{L}_0(u^{n+1}) = \mathcal{L}_0(u^n) - \mathcal{L}(u^n) - f(u^n), \tag{7}$$

The resulting linear system

$$(\frac{1}{\Delta t} - \epsilon^2 \Delta + S) u^{n+1} = g^n \tag{8}$$

can be solved efficiently with FFT.

The situation is slightly different for the fractional model (1) if we take

$$\mathcal{L}_0 u = \epsilon^2 (-\Delta)_{\mathrm{R}}^{\alpha/2} u + Su, \tag{9}$$

as the corresponding linear system

$$(\frac{1}{\Delta t} + \epsilon^2 (-\Delta)_{\mathrm{R}}^{\alpha/2} + S) u^{n+1} = g^n \tag{10}$$

does not have a fast direct solver. Either an efficient preconditioner for the fractional operator $C + \epsilon^2(-\Delta)_{\mathrm{R}}^{\alpha/2}$, or further splitting of the term $\epsilon^2(-\Delta)_{\mathrm{R}}^{\alpha/2}$ is required:

$$\mathcal{L}_0 u = \epsilon^2 C \mathbb{M} u + Su, \tag{11}$$

where $\mathbb{M}$ in (11) can be taken as a preconditioner, if available. The splitting (9) results in a preconditioned iterative scheme and the (11) results in a direct scheme provided a suitable splitting $\mathbb{M}$ is found. In previous MoST project, we found that the spectral fractional Laplacian $\mathbb{M} = (-\Delta)_{\mathrm{S}}^{\alpha/2}$ can be solved by FFT and serves as an extremely good preconditioner and can be applied in both approaches (9) or (11). See section 1.1 and 4.1 for details.

There have been several generalization of the stabilization to higher order schemes. A well known 2nd order time discretization combines Crank-Nicolson method for $\mathcal{L}_0(u)$ together with 2nd order Adam-Bashforth for $\mathcal{L}(u) - \mathcal{L}_0(u)$ to get (CN-AB2)

$$\frac{u^{n+1}-u^n}{\Delta t} + \mathcal{L}_0(\frac{u^{n+1}+u^n}{2}) = \frac{3}{2}\big(\mathcal{L}_0(u^n) - \mathcal{L}(u^n - f(u^n))\big) - \frac{1}{2}\big(\mathcal{L}_0(u^{n-1}) - \mathcal{L}(u^{n-1} - f(u^{n-1}))\big) \tag{12}$$

In this MoST proposal, we consider an alternative stabilized semi-implicit second order scheme (also known as predictor-corrector scheme [38]):

$$\begin{cases} \dfrac{u^{n+\frac{1}{2}} - u^n}{\frac{\Delta t}{2}} + \mathcal{L}_0(u^{n+\frac{1}{2}}) = (\mathcal{L}_0 - \mathcal{L})(u^n) - f(u^n) \\ \dfrac{u^{n+1} - u^n}{\Delta t} + \mathcal{L}_0(\dfrac{u^{n+1}+u^n}{2}) = (\mathcal{L}_0 - \mathcal{L})(u^{n+\frac{1}{2}}) - f(u^{n+\frac{1}{2}}) \end{cases} \tag{13}$$

Due to the presence of intermediate step $u^{n+\frac{1}{2}}$ in the scheme (13), sharp stability estimate is difficult to obtain in general. It is well believed that the system is stabilized as long as the stabilizing term $\mathcal{L}_0$ is large enough. On the other hand, we have observed that the overall absolute error also increases with $\mathcal{L}_0$.

For general (possibly nonlinear or nonlocal) elliptic operator $\mathcal{L}u + f(u)$, the second order scheme (13) is a natural generalization of (6) and retains all the numerical advantages. Both steps in (13) are uniquely solvable with fast solvers provided $\mathcal{L}_0$ is a suitable chosen constant coefficient elliptic operator. The stability of (13) is not clear in general. Numerical evidence in [38] (and rigorous proof in some cases) suggests that (13) is more robust and accurate for gradient flows with strong anisotropic free energy. We believe this is due to lack of extrapolation steps in (13). In a preliminary analysis, we start with the the simplest case where $\mathcal{L}$ is linear nonnegative self-adjoint, $f = 0$ and found a precise sufficient condition on the stabilizing term $\mathcal{L}_0$ for the scheme (13) to be unconditional stable (see section 4.3). We believe this is a strong indication for nonlinear stability of the stabilized scheme (13) and will also pursue in this direction for the current MoST proposal.

2.1 Potential difficulties and proposed method of resolution

In contrast to classical integer order PDEs, the main difficulty associated with numerical computations of (10) is that these operators are non-local, hyper-singular integral operators. To solve (10) accurately and efficiently, the central issues include:

(a) Accurate discretization of (10).

(b) Fast evaluation of matrix-vector multiplication corresponding to the discretization of (10).

(c) Efficient preconditioning technique for the linear system resulting from (a), (b).

We will elaborate them in the following subsections. To simplify the presentation, we will mainly explain these issues in the 1D setting (that is $d = 1$, $\Omega = [a, b]$) and comment briefly in the multi-dimensional case.

2.1.1 Accurate Structure Preserving Discretizations

Since (10) is a nonlocal operator, standard numerical discretization of the fractional Laplacian (10) inevitably leads to a **dense matrix**. This poses a main difficulty in all iterative solvers as the matrix-vector multiplication is extremely expensive. Moreover, since the integral in (10) is hyper-singular, a proper regularization procedure is required to evaluate the integral accurately.

On the other hand, the fractional Laplace operator is translation-invariant. If the translation invariant property can be preserved numerically at the discrete level, the corresponding discrete fractional Laplace operator gives rise to a **Toeplitz matrix**, thus the matrix-vector multiplication in (10) can be performed efficiently by FFT with $O(N \log N)$ complexity.

The discrete translation-invariant property of (10) (and hence the Toeplitz structure) is possible only on uniform grids. We will thus restrict our discussion in this class of discretizations. Here we list a few known discretizations along this line:

1. One of the most widely adopted structure preserving spatial discretization is based on the identity
$$\mathrm{PV}\int_a^b \frac{u(x)-u(y)}{|x-y|^{1+\alpha}}dy = \frac{{}_{-\infty}\partial_x^\alpha u(x) + {}_x\partial_\infty^\alpha u(x)}{2\cos(\alpha\pi/2)} \tag{14}$$
for smooth enough u, and the the Grünwald Letnikov formula (the Grünwald approximation) for the left Riemann-Liouville fractional derivative ${}_{-\infty}\partial_x^\alpha$ (with the understanding that $u=0$ on $x<a$):
$${}^{\mathrm{GL}}_{a}\partial_x^\alpha u(x) = \lim_{N\to\infty}\frac{1}{h^\alpha}\sum_{k=0}^{N}(-1)^k\binom{\alpha}{k}u(x-kh) \tag{15}$$
where N is the number of partition and $h=(x-a)/N$. A stable right-shifted approximation of the the Grünwald Letnikov formula (15) is proposed in [30] which leads to a Toeplitz matrix with $O(h)$ discretization error for the left Riemann-Liouville fractional derivative
$$G = \frac{1}{h^\alpha}\begin{bmatrix} g_1^\alpha & g_0^\alpha & 0 & \cdots & 0 \\ g_2^\alpha & g_1^\alpha & g_0^\alpha & \cdots & 0 \\ \vdots & \ddots & \ddots & \ddots & \vdots \\ g_{N-2}^\alpha & \ddots & \ddots & \ddots & g_0^\alpha \\ g_{N-1}^\alpha & g_{N-2}^\alpha & \cdots & \cdots & g_1^\alpha \end{bmatrix}$$
where $g_0^\alpha = 1$,
$$g_k^\alpha = \frac{-(\alpha-k+1)}{k}g_{k-1}^\alpha$$
and $h=(b-a)/N$. A similar formula for ${}_x\partial_\infty^\alpha u(x)$ leads to the matrix representation for the right Riemann-Liouville fractional derivative G^T.

   The Grünwald approximation is later improved to second order accurate in [39] by way of a weighted and shifted combination of the first order Grünwald approximation, retaining the Toeplitz structure. In addition to the Riesz fractional Laplacian, this discretization can be generalized to variable coefficient Riemann-Liouville fractional PDEs, the fractional diffusion operator can thus be represented by a linear combination of diagonal-times-Toeplitz matrices, and therefore the matrix-vector multiplication can be performed efficiently by FFT with $O(N\log N)$ complexity. As a consequence, almost all the earlier works in 1D adopt these Grünwald discretizations. However, it is not clear how to generalize the Grünwald approximation to the multi-dimensional fractional Laplacian.

2. More recent structure preserving discretization of the fractional Laplacian are mostly based on the Riesz representation (10). In ([21]), Huang and Oberman proposed to

discretize the operator by dividing the integral in to singular and regular parts. For the singular part, the authors use Taylor expansion and finite difference approximation for $|y| \leq h$. For the regular part $|y| \geq h$, they approximate the integrand by standard polynomial interpolant. This results an 2nd order approximation of (10) with a Toeplitz matrix.

3. In [13] Duo, van Wyk and Zhang discretized the Riesz fractional Laplacian by introducing a splitting parameter and formulate the fractional Laplacian as the weighted integral, then approximated it by weighted trapezoidal rule. The results is also 2nd order accurate a and leads to a Toeplitz matrix.

4. In [33] Minden and Ying discretized the fractional Laplacian by subtracting a polynomial times a cut off function to remove the singular part, then using trapezoidal rule for the smooth part and finite difference approximation of the derivative for the remaining part. The results is also 2nd order accurate a and leads to a Toeplitz matrix and applies to multi-dimensional case. So far, this scheme appears to be the only structure preserving discretization in multi-dimension.

5. In previous MoST project, we have develop a novel spatial discretization that can be upgraded to 4th order in space very easily. See section 4.2 for details

2.1.2 Efficient Preconditioners for solving the Toeplitz-like matrices

In the constant coefficient case, the 1D fractional diffusion equation results in exact Toeplitz matrices (with Backward Euler or higher order implicit time discretization). The fast iterative solver for Toeplitz matrices is very well developed, see [9] for a thorough review.

For the variable coefficient case, the resulting matrices are combinations of diagonal-times-Toeplitz matrices. Most existing preconditioners fall into two categories:

- Circulant preconditioners as in [25, 34, 26].
- Banded matrix preconditioners as in [42, 43, 22, 28, 48].

In previous MoST project (2019/08/01-2020/07/31), we proposed a novel preconditioner based on the spectral fractional Laplacian (2). Note that the spectral fractional Laplacian and the Riesz fractional Laplacian (10) are genuinely different operators. Nevertheless, numerical evidence shows that they are spectrally equivalent. Moreover, the spectral fractional Laplacian be easily inverted using Fast Discrete Sine Transform and serves as a perfect candidate of the preconditioner both in 1D and multi-dimensional cases. The results so far are summarized in Appendix 4.1.

3 Conclusion

The fractional order PDE is a fast growing research subject on many aspects including theory, numeric and applications. Unlike classical PDEs, the fractional PDE can describe a wider range of phenomenon which are important in many branches of science and engineering. In this MoST proposal, we expect to be able to develop fast efficient numerical schemes for the fractional model (fisac 1) and conduct rigorous error analysis. Graduate students and postdocs will definitely benefit significantly from participating this project.

References

AlCa79 [1] Allen, S.M., Cahn, J.W.: A microscopic theory for antiphase boundary motion and its application to antiphase domain coarsening. Acta Metall. 27, 1085–1095 (1979)

AiMa17a [2] M. Ainsworth and Z. Mao, Analysis and Approximation of a Fractional Cahn-Hilliard Equation, SIAM J. Numer. Anal., 55 (4) (2017) pp. 1689-1718. doi:10.1137/16M1075302.

AiMa17b [3] M. Ainsworth and Z. Mao, Well-posedness of the Cahn-Hilliard equation with fractional free energy and its Fourier Galerkin approximation, Chaos Solitons Fractals, 102 (2017) pp. 264-273. doi:10.1016/j.chaos.2017.05.022.

AkScSe16 [4] G. Akagi, G. Schimperna, and A. Segatti, Fractional Cahn-Hilliard, Allen-Cahn and porous medium equations, J. Differ. Equ., 261 (6) (2016) pp. 2935-2985. doi:https://doi.org/10.1016/j.jde.2016.05.016.

AnMaRoTo10 [5] F. Andreu, J. M. Mazon, J. D. Rossi, and J. Toledo, Nonlocal diffusion problems, Math. Surveys Monogr. 165, AMS, Providence, RI, 2010.

BuKaBu14 [6] Bueno-Orovio, A., Kay, D., Burrage, K., Fourier spectral methods for fractional-in-space reaction diffusion equations. BIT Numer. Math. 54(4), 937–954 (2014)

BuHaKa12 [7] Burrage, K., Hale, N., Kay, D., An efficient implicit FEM scheme for fractional-in-space reaction-diffusion equations. SIAM J. Sci. Comput. 34, A2145–A2172 (2012)

BuVa16 [8] C. Bucur and E. Valdinoci, Nonlocal diffusion and applications, Vol. 20. Bologna: Springer, 2016.

ChNg96 [9] R. H. Chan and M. K. Ng, Conjugate gradient methods for Toeplitz systems, SIAM Rev., 38 (3) (1993) pp. 427-482.

ChHo04 [10] W. Chen and S. Holm, Fractional Laplacian time-space models for linear and nonlinear lossy media exhibiting arbitrary frequency power-law dependency, J. Acoust. Soc. Am., 115(4): pp. 1424-1430, 2004.

a4 [11] Choi, J.W., Lee, H.G., Jeong, D., Kim, J. An unconditionally gradient stable numerical method for solving the Allen–Cahn equation. Phys. A Stat. Mech. Appl. 388(9), 1791–1803 (2009)

CoWu99 [12] P. Constantin and J. Wu, Behavior of solutions of 2D quasi-geostrophic equations, SIAM J. Math. Anal. 30 (5) (1999) pp. 937-948. doi:10.1137/S0036141098337333.

DuWyZh18 [13] S. Duo, H. W. van Wyk, and Y. Zhang, A novel and accurate finite difference method for the fractional Laplacian and the fractional Poisson problem, J. Comput. Phys. 355 (2018): 233-252.

Ey98 [14] D. J. Eyre, Unconditionally gradient stable time marching the Cahn-Hilliard equation, in: Computational and Mathematical Models of Microstructural Evolution, San Francisco, CA, 1998, in Mater. Res. Soc. Symp. Proc., vol.529, MRS, Warrendale, PA, 1998, pp. 39-46

a7 [15] Feng, X., Prohl, A., Numerical analysis of the Allen–Cahn equation and approximation for mean curvature flows. Numer. Math. 94(1), 33–65 (2003)

a8 [16] Feng, X., Song, H., Tang, T., Yang, J., Nonlinear stability of the implicit–explicit methods for the Allen–Cahn equation. Inverse Probl. Imaging 7, 679–695 (2013)

a9 [17] Feng, X.,Tang,T.,Yang, J., Stabilized Crank–Nicolson/Adams–Bashforth schemes for phase field models. East Asian J. Appl. Math. 3, 59–80 (2013)

HoTaYa17 [18] T. Hou, T. Tang, and J. Yang, Numerical analysis of fully discretized Crank¡Nicolson scheme for fractional-in-space Allen-Cahn equations, J. Sci. Comput. 72.3 (2017): 1214-1231.

a10 [19] Kim, J., Phase-field models for multi-component fluid flows. Commun. Comput. Phys. 12, 613–661 (2012)

a16 [20] Shen, J., Yang, X., Numerical approximations of Allen–Cahn and Cahn–Hilliard equations. Discret. Contin. Dyn. Syst. 28, 1669–1691 (2010)

HuOb14 [21] Y. Huang, and A. Oberman, Numerical methods for the fractional Laplacian: A finite difference-quadrature approach, SIAM J.Numer. Anal 52.6 (2014): 3056-3084.

JiLiZh15 [22] X. Q. Jin, F. R. Lin, and Z. Zhao, Preconditioned iterative methods for two-dimensional space-fractional diffusion equations, Commun Comput Phys. 18.2 (2015): pp. 469-488.

Kw17 [23] M. Kwaśnick, Ten equivalent definitions of the fractional Laplace operator, Fract. Calc. Appl. Anal., 20 (1) (2017) pp. 7-51. doi:10.1515/fca-2017-0002.

La00 [24] N. Laskin, Fractional quantum mechanics and Lévy path integrals, Phys. Lett., A 268 (4) (2000) pp. 298-305. doi:10.1016/S0375-9601(00)00201-2.

LeSu13 [25] S.-L. Lei, and H.-W. Sun, A circulant preconditioner for fractional diffusion equations, J. Comput. Phys. 242 (2013): 715-725.

LiNgSu17 [26] X.-L. Lin, M. Ng, and H.-W. Sun, A splitting preconditioner for Toeplitz-like linear systems arising from fractional diffusion equations, SIAM J. Matrix Anal. Appl. 38.4 (2017): pp. 1580-1614.

Li_etal18 [27] A. Lischke, G. Pang, M. Gulian, F. Song, C. Glusa, X. Zheng, Z. Mao, W. Cai, M. Meerschaert, M. Ainsworth, and G. Karniadakis, What Is the Fractional Laplacian?, arXiv preprint arXiv:1801.09767 (2018).

LiYaJi14 [28] F. R. Lin, S. W. Yang, and X. Q. Jin, Preconditioned iterative methods for fractional diffusion equation, J. Comput. Phys. 256 (2014): pp. 109-117.

Li13 [29] J. Liu, Simple and efficient ALE methods with provable temporal accuracy up to fifth order for the Stokes equations on time varying domains, SIAM J. Numer. Anal. 51.2 (2013): 743-772.

MeTa04 [30] M. Meerschaert and C. Tadjeran, Finite difference approximations for fractional advection-dispersion flow equations, J. Comput. Appl. Math 172.1 (2004): pp. 65-77.

MeTa06 [31] M. Meerschaert and C. Tadjeran, Finite difference approximations for two-sided space-fractional partial differential equations, Appl. Numer. Math., 56.1 (2006): pp. 80-90.

MeSi11 [32] M. Meerschaert and A. Sikorskii, Stochastic Models for Fractional Calculus, Walter De Gruyter, 2011.

MiYi18 [33] V. Minden, and L. Ying, A simple solver for the fractional Laplacian in multiple dimensions, arXiv preprint arXiv:1802.03770 (2018).

PaKeNgSu14 [34] J. Pan, R. Ke, M. Ng, and H.-W. Sun , Preconditioning techniques for diagonal-times-Toeplitz matrices in fractional diffusion equations SIAM J. Sci. Comput. 36.6 (2014): pp. A2698-A2719.

PaQuRoVa11 [35] A. de Pablo, F. Quirós, A. Rodríguez, and J. Vázquez, A fractional porous medium equation, Adv. Math., 226 (2) (2011) pp. 1378-1409. doi:10.1016/j.aim.2010.07.017.

Po16 [36] C. Pozrikidis, The fractional Laplacian, CRC Press, Boca Raton, FL, 2016.

ShWaWaWi12 [37] J. Shen, C. Wang, X. Wang, and S. M. Wise, Second-order convex splitting schemes for gradient flows with Ehrlich-Schnabel type energy: application to thin film epitaxy, SIAM J. Numer. Anal. 50.1 (2012): 105-125.

ShXu18b [38] J. Shen and J. Xu, Stabilized predictor-corrector schemes for gradient flows with strong anisotropic free energy, Commun. Comput. Phys., 24 (2018): 635-654.

TiZhDe15 [39] W. Y. Tian, H. Zhou, and W. Deng, A class of second order difference approximations for solving space fractional diffusion equations, Math. Comput. 84.294 (2015): pp. 1703-1727.

TrCo10 [40] B. Treeby and B. Cox, Modeling power law absorption and dispersion for acoustic propagation using the fractional Laplacian, J. Acoust. Soc. Am., 127 (5) (2010) pp. 2741-2748. doi:10.1121/1.3377056.

Va17 [41] J. Vázquez, The mathematical theories of diffusion Nonlinear and fractional diffusion, in: Nonlocal and Nonlinear Diffusions and Interactions: New Methods and Directions, Springer, 2017, pp. 205-278.

WaWaSi10 [42] H. Wang, K. Wang, and T. Sircar, A direct $O(N \log^2 N)$ finite difference method for fractional diffusion equations, J. Comput. Phys. 229.21 (2010): pp. 8095-8104.

WaWa11 [43] H. Wang and K. Wang, An $O(N \log^2 N)$ alternating-direction finite difference method for two-dimensional fractional diffusion equations, J. Comput. Phys. 230.21 (2011): pp. 7830-7839.

XuTa06 [44] C. Xu, and T. Tang, Stability analysis of large time-stepping methods for epitaxial growth models, SIAM J. Numer. Anal. 44.4 (2006): 1759-1779.

Ya02 [45] M. Yamamoto, Asymptotic expansion of solutions to the dissipative equation with fractional Laplacian, SIAM J. Math. Anal., 44 (6) (2012) pp. 3786-3805. doi:10.1137/120873200.

a20 [46] Yang, X., Error analysis of stabilized semi-implicit method of Allen–Cahn equation. Discrete Contin. Dyn. Syst. Ser. B 11(4), 1057–1070 (2009)

a23 [47] Zhang, J., Du, Q., Numerical studies of discrete approximations to the Allen–Cahn equation in the sharp interface limit. SIAM J. Sci. Comput. 31(4), 3042–3063 (2009)

ZhJiLi16 [48] Z. Zhao, X. Q. Jin, and M. M. Lin, Preconditioned iterative methods for space-time fractional advection-diffusion equations, J. Comput. Phys. 319 (2016): pp. 266-279.

4 Appendix

4.1 Result of the previous MoST project (2019/08/01-2021/01/31)

A2old , In this section, we report our progress of the MoST project on efficient preconditioner for the structure preserving discretization of the Riesz fractional Laplacian (be3n 10).

The novelty of our approach is to use the spectral fractional Laplacian as the preconditioning operator for various discretizations described in section known_disc 2.1.1.

More precisely, consider the standard discrete Laplacian

$$-\Delta_h = \frac{1}{h^2}\begin{bmatrix} 2 & -1 & & & \\ -1 & 2 & -1 & & \\ & \ddots & \ddots & \ddots & \\ & & -1 & 2 & -1 \\ & & & -1 & 2 \end{bmatrix} = P\Lambda P^{-1}$$

where

$$P = \begin{bmatrix} \sin(\frac{\pi}{N}) & \sin(\frac{2\pi}{N}) & \dots & \sin(\frac{(N-1)\pi}{N}) \\ \sin(\frac{2\pi}{N}) & \sin(\frac{4\pi}{N}) & \dots & \sin(\frac{2(N-1)\pi}{N}) \\ \vdots & \vdots & & \vdots \\ \sin(\frac{(N-1)\pi}{N}) & \sin(\frac{2(N-1)\pi}{N}) & \dots & \sin(\frac{(N-1)^2\pi}{N}) \end{bmatrix}$$

and

$$\Lambda = \frac{1}{(\frac{L}{N})^2} \begin{bmatrix} (2\sin\frac{\pi}{2N})^2 & & & \\ & (2\sin\frac{2\pi}{2N})^2 & & \\ & & \ddots & \\ & & & (2\sin\frac{(N-1)\pi}{2N})^2 \end{bmatrix}$$

Here, the diagonal entries of Λ are the eigenvalues of $(-\Delta_h)$. Thus the discrete spectral fractional Laplacian is given by

$$(-\Delta_{\mathrm{S},h})^{\alpha/2} = P\Lambda^{\frac{\alpha}{2}}P^{-1}$$

where

$$\Lambda^{\frac{\alpha}{2}} = \frac{1}{(\frac{L}{N})^\alpha} \begin{bmatrix} (2\sin\frac{\pi}{2N})^\alpha & & & \\ & (2\sin\frac{2\pi}{2N})^\alpha & & \\ & & \ddots & \\ & & & (2\sin\frac{(N-1)\pi}{2N})^\alpha \end{bmatrix}$$

From the construction of $(-\Delta_{\mathrm{S},h})^{\alpha/2}$, it is clear that the computational cost for solving the linear system $(-\Delta_{\mathrm{S},h})^{\alpha/2}x = b$ is $O(N \log N)$ via Fast Discrete Sign Transform.

We therefore take

$$M = (-\Delta_{\mathrm{S},h})^{\alpha/2}$$

as the preconditioner for the matrices resulting from various discretizations of the Riesz operator described in section known_disc 2.1.1:

- A_{HO}: the Huang-Oberman discretization HuOb14 [21].
- A_{sG}: the second order shifted Grünwald discretization TiZhDe15 [39].
- A_{DWZ}: the Duo-van Wyk-Zhang discretization DuWyZh18 [13].
- A_{MY}: the Minden-Ying discretization MiYi18 [33].

Example 1: In this example, we solve for u from

$$Au = f$$

where $u = (1-x^2)^{s+\frac{\alpha}{2}}$, $f = \frac{2^\alpha \Gamma(\frac{\alpha+1}{2})\Gamma(s+1+\frac{\alpha}{2})}{\sqrt{\pi}\Gamma(s+1)} {}_2F_1(\frac{\alpha+1}{2}, -s; \frac{1}{2}; x^2)$, $s = 3$ and A is any of the matrices listed above. We solve it iteratively with CG or PCG using $M = (-\Delta_{\mathrm{S},h})^{\alpha/2}$ described above as the preconditioner. The results are summarized in Table steady_state_iter 1.

Table 1: Iteration numbers of Example 1: Plain: PCG, preconditioned by M. Parenthesis: CG, no preconditioners.

steady_state_iter

scheme	α	N= 32	N= 128	N= 512	N= 2048
HO[21]	1.1	8(15)	8(40)	8(88)	9(191)
HO[21]	1.5	7(16)	7(55)	7(163)	8(466)
HO[21]	1.9	5(16)	5(64)	6(250)	6(942)
sG[39]	1.1	10(13)	11(32)	11(72)	12(157)
sG[39]	1.5	9(16)	10(48)	11(139)	11(398)
sG[39]	1.9	6(16)	7(64)	7(241)	8(900)
DWZ[13]	1.1	6(16)	7(42)	7(93)	7(202)
DWZ[13]	1.5	6(16)	6(58)	7(170)	7(486)
DWZ[13]	1.9	5(16)	5(64)	6(252)	6(950)
MY[33]	1.1	7(16)	7(43)	8(96)	8(207)
MY[33]	1.5	7(16)	7(59)	7(173)	8(493)
MY[33]	1.9	5(16)	5(64)	6(253)	6(953)

Example 2: In this example, we perform similar test on two dimensional case using example in [33] on $\Omega \in [0,1]^2$. The preconditioner $M = (-\Delta_{S,h})^{\alpha/2}$ can be easily generalized to rectangular domains $[0,1]^d \subset \mathbf{R}^d$ and inverted with $O(N \log N)^d$ operations. Note that [33] is the only structure preserving discretization in multi-dimensional case and our proposed preconditioner $M = (-\Delta_{S,h})^{\alpha/2}$ clearly outperforms the preconditioner proposed by the authors in [33]. The results are summarized in table 2.

4.2 Progress in ongoing MoST Proposal (2020/08/01-2021/07/31), officially extended to 2022/07/31: Structure Preserving Discretization with Integrable Singular Convolution Kernel

TW4

In this ongoing MoST project, the PI is conducting research on higher order structure preserving discretization of the fractional Laplacian for (10) in multi-dimensions. The first novelty of our method is to utilize the identity

$$c(n,\alpha)\text{P.V.}\int_{\mathbf{R}^n} \frac{u(x)-u(y)}{|x-y|^{d+\alpha}}dy = C(d,\alpha-2)\Delta \int \frac{u(y)}{|x-y|^{d+\alpha-2}}dy, \qquad (16)$$

id2

which provides yet another equivalent formulation for $(-\Delta)^{\frac{\alpha}{2}}u$.

From the numerical point of view, the new equivalent formula, the right hand side of (16), possesses significance advantages over the left hand side, the Riesz formula:

(i) On the integral part, the kernel of the right hand side is two orders more regular than that of the left hand side (**and is integrable**). Desingularization and higher order quadrature can be achieved more easily with the new approach described below.

Table 2: Iteration numbers of Example 2: Plain: PCG, preconditioned by $M = (-\Delta_{S,h})^{\alpha/2}$. Bracket: PCG with preconditioner proposed in [33]. Parenthesis: CG, no preconditioners.

pre_num_ying

α	N	tol=10^{-6}	tol=10^{-9}
1.25	128	6[21](61)	9[33](77)
1.25	256	7[28](95)	9[43](121)
1.25	512	7[36](148)	10[57](188)
1.25	1024	7[47](231)	10[74](292)
1.5	128	6[15](86)	8[23](108)
1.5	256	6[18](147)	9[28](184)
1.5	512	7[21](250)	9[33](312)
1.5	1024	7[26](425)	10[40](528)
1.75	128	5[11](120)	7[15](149)
1.75	256	5[12](223)	7[17](278)
1.75	512	6[13](413)	8[19](516)
1.75	1024	6[14](766)	8[21](962)

(ii) If u is regular enough, standard higher order discretization can be applied to the standard Laplacian outside of the integration on the right hand side.

(iii) Both (i) and (ii) can be carried out with structure preserving discretizations, leading to a Toeplitz-like linear system that can be evaluated and solved with $O(N \log N)^d$ operations.

The second key ingredient of our method is a new treatment of mild integrable singularity. Take the 1D case for example. The right hand side of (16) gives:

$$
\begin{aligned}
(-\Delta)^{\frac{\alpha}{2}} u(x_k) =& \frac{1}{2\cos(\frac{\alpha\pi}{2})} \frac{d^2}{dx^2} \int_a^b \frac{u(s)}{|x_k - s|^{\alpha-1}} ds \\
=& \frac{1}{2\cos(\frac{\alpha\pi}{2})} \frac{d^2}{dx^2} \sum_j \int_{I_j} \frac{u(s)}{|x_k - s|^{\alpha-1}} ds
\end{aligned}
$$

where $I_j = [x_{j-\frac{1}{2}}, x_{j+\frac{1}{2}}]$.

Instead of using the standard quadrature rule:

$$
\int_{I_j} \frac{u(s)}{|x_k - s|^{\alpha-1}} ds \approx w_i \frac{u(s_i)}{|x_k - s_i|^{\alpha-1}} |I_j|
$$

which only gives $O(h^{2-\alpha})$ overall accuracy of integration due to the mild singularity at $j \sim k$, we take the following approach to separate the singularity:

We observe that, if u is smooth, we can approximate the integral in each I_j by

$$u(s) = u(x_i) + D_h u(x_i)(s - x_i) + \frac{D_h^2 u(x_i)}{2}(s - x_i)^2 + O(h^3) \text{ on } I_j \tag{17}$$

q0

and

$$\int_{I_j} \frac{u_j(s)}{(x_k - s)^{\alpha-1}} ds \approx K_{k-j}^{(0)} u(x_j) + K_{k-j}^{(1)} D_h u(x_j) + K_{k-j}^{(2)} \frac{D_h^2 u(x_j)}{2} \tag{18}$$

q1

where

$$K_{k-j}^{(i)} = \int_{I_j} \frac{(s - x_j)^i}{(x_k - s)^{\alpha-1}} ds$$

Overall, the formula (18) results in an Toeplitz matrix with 4th order accurate for smooth solutions.

Figure 1:

curv

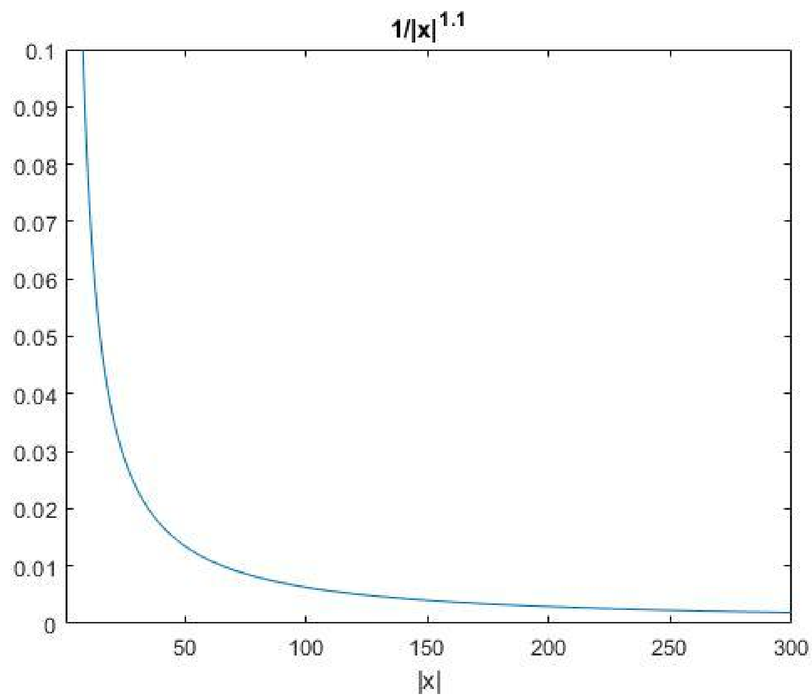

To compute the Toeplitz kernel $\int_{I_j} \frac{(s - x_j)^i}{(x_k - s)^{\alpha-1}} ds$, it suffices to evaluate it using standard Gaussian quadrature. Away from the singularities, 3 Gaussian quadrature points in each direction (9 quadrature points in each 2D cell) is enough to provide machine accuracy. The number of quadrature points is increased as we approach the singularity. Since the singular region only constitutes a small portion of the computational domain, the overall

Figure 2:

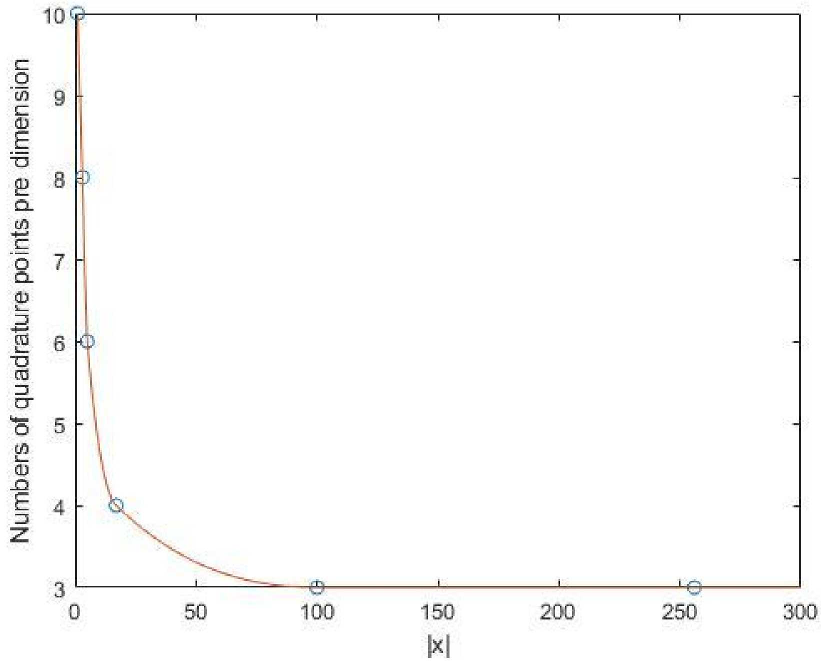

computational cost only increases by a small fraction compared to the quadrature for smooth regions. Figure 1 and Figure 2 demonstrate the number of quadrature points needed in each dimension as a function of distance to the singularity. Average number of quadrature points per cell is around 3.15^2 for an $N \times N$ simulation with $N = 256$ (or 10% increase in computational cost compared to 3^2 quadrature points per cell on smooth regions). Obviously the average cost per cell decreases as N in creases.

We have successfully developed a novel structure preserving discretization which is 4th order accurate for smooth solutions in 1D and 2D. The computational cost for evaluating the convolution kernel is $O(N)$ in 1D and $O(N^2)$ in 2D. where N is the number of partitions in each direction. With the built-in Toeplitz structure, the evaluation of the convolution (matrix-vector multiplication) is $O(N \log N)$ in 1D and $O(N \log N)^2$ in 2D. The 3D code is currently under development.

4.3 Stability Analysis of for linear Systems

We first rewrite the linear system

$$u_t = -\mathcal{L}(u) + f \tag{19}$$

after spatial discretization, in matrix and vector notations:

$$\boldsymbol{u}_t + C_1 \mathbb{M} \boldsymbol{u} = (C_1 \mathbb{M} - \mathbb{A}) \boldsymbol{u} + \boldsymbol{f} \tag{20}$$

Here $\boldsymbol{u}$ and $\boldsymbol{f}$ are vector valued grid functions, in $\mathbf{R}^{M-1}$. Denote by

$$\mathbb{A}: \text{ matrix representation of } \mathcal{L}, \qquad C_1\mathbb{M}: \text{ matrix representation of } \mathcal{L}_0$$

$\mathbb{M}$ and $\mathbb{A}$ are real $(M-1)\times(M-1)$ real matrices. By assumption $\mathbb{M} = \mathbb{M}^{\mathrm{T}} > 0, \mathbb{A} = \mathbb{A}^{\mathrm{T}} > 0$. In practice, we can take $\mathbb{M}$ to be a preconditioner of $\mathbb{A}$, if available and C_1 is a constant to be determined.

For two real symmetric $(M-1)\times(M-1)$ matrices $\mathbb{P}$ and $\mathbb{Q}$, we write $\mathbb{P} > \mathbb{Q}$ provided $\boldsymbol{u}^{\mathrm{T}}\mathbb{P}\boldsymbol{u} > \boldsymbol{u}^{\mathrm{T}}\mathbb{Q}\boldsymbol{u}$ for all $\boldsymbol{u} \in \mathbf{R}^{M-1} \setminus \{\mathbf{0}\}$. Similarly for $\mathbb{P} \geq \mathbb{Q}$. We also denote the standard L^2 and weighted inner products and norms in $\mathbf{R}^{M-1}$ for any $\mathbb{W} = \mathbb{W}^{\mathrm{T}} \geq 0$ by

$$\langle \boldsymbol{u}, \boldsymbol{v} \rangle = \boldsymbol{u}^{\mathrm{T}}\boldsymbol{v}, \qquad \langle \boldsymbol{u}, \boldsymbol{v} \rangle_{\mathbb{W}} = \boldsymbol{u}^{\mathrm{T}}\mathbb{W}\boldsymbol{v}, \tag{21}$$

and

$$\|\boldsymbol{u}\|^2 = \langle \boldsymbol{u}, \boldsymbol{u} \rangle, \qquad \|\boldsymbol{u}\|_{\mathbb{W}}^2 = \langle \boldsymbol{u}, \boldsymbol{u} \rangle_{\mathbb{W}}. \tag{22}$$

4.3.1 Stabilized Backward Euler Scheme

aos1

In the matrix vector notation, the stabilized Backward Euler method (6) reads

$$\frac{\boldsymbol{u}^{n+1} - \boldsymbol{u}^n}{\Delta t} + C_1\mathbb{M}\boldsymbol{u}^{n+1} = (C_1\mathbb{M} - \mathbb{A})\boldsymbol{u}^n + \boldsymbol{f}^n, \tag{23}$$ be2

We will show that (23) are stable both in energy norm and L^2 norm. The argument is straight forward, see also [44], for example. We include it here for readers convenience in reading section 4.3.2.

thmbe1 **Theorem 1.** *If $C_1\mathbb{M} \geq \frac{1}{2}\mathbb{A}$, then the stabilized backward Euler scheme (23) is unconditionally stable and satisfies*

$$\|\boldsymbol{u}^N\|_{\mathbb{A}}^2 \leq \|\boldsymbol{u}^0\|_{\mathbb{A}}^2 + \frac{\Delta t}{2}\sum_{n=1}^{N-1}\|\boldsymbol{f}^n\|^2 \tag{24}$$ aest

and

$$\|\boldsymbol{u}^N\|^2 + \Delta t\|\boldsymbol{u}^N\|_{C_1\mathbb{M}-\frac{\mathbb{A}}{2}}^2 \leq \|\boldsymbol{u}^0\|^2 + \Delta t\|\boldsymbol{u}^0\|_{C_1\mathbb{M}-\frac{\mathbb{A}}{2}}^2 + \frac{\Delta t}{2}\sum_{n=0}^{N-1}\|\boldsymbol{f}^n\|_{\mathbb{A}^{-1}}^2 \tag{25}$$ l2es

Proof.

$$\mathbb{Q} \equiv \left(\frac{1}{\Delta t} + C_1\mathbb{M}\right). \tag{26}$$ def0

and rewrite (23)

$$\mathbb{Q}(\boldsymbol{u}^{n+1} - \boldsymbol{u}^n) + \mathbb{A}\boldsymbol{u}^n = \boldsymbol{f}^n \tag{27}$$ BE3

Take $\langle \boldsymbol{u}^{n+1} - \boldsymbol{u}^n, \bullet \rangle$ on both sides of (27), and write $\mathbb{A}\boldsymbol{u}^n = \frac{1}{2}\mathbb{A}(\boldsymbol{u}^{n+1} + \boldsymbol{u}^n) - \frac{1}{2}\mathbb{A}(\boldsymbol{u}^{n+1} - \boldsymbol{u}^n)$, we have

$$\|\boldsymbol{u}^{n+1} - \boldsymbol{u}^n\|_{\mathbb{Q}}^2 - \frac{1}{2}\|\boldsymbol{u}^{n+1} - \boldsymbol{u}^n\|_{\mathbb{A}}^2 + \frac{1}{2}\left(\|\boldsymbol{u}^{n+1}\|_{\mathbb{A}}^2 - \|\boldsymbol{u}^n\|_{\mathbb{A}}^2\right) = \langle \boldsymbol{u}^{n+1} - \boldsymbol{u}^n, \boldsymbol{f}^n \rangle \tag{28}$$

or

$$\|\boldsymbol{u}^{n+1}-\boldsymbol{u}^n\|^2_{\mathbb{Q}-\frac{\mathbb{A}}{2}}+\frac{1}{2}\left(\|\boldsymbol{u}^{n+1}\|^2_{\mathbb{A}}-\|\boldsymbol{u}^n\|^2_{\mathbb{A}}\right)=\langle\boldsymbol{u}^{n+1}-\boldsymbol{u}^n,\boldsymbol{f}^n\rangle \tag{29}$$

From (26), we have

$$\|\cdot\|^2_{\mathbb{Q}-\frac{\mathbb{A}}{2}}=\frac{1}{\Delta t}\|\cdot\|^2+\|\cdot\|^2_{C_1\mathbb{M}-\frac{\mathbb{A}}{2}} \tag{30}$$

From (30), we have

$$\frac{1}{\Delta t}\|\boldsymbol{u}^{n+1}-\boldsymbol{u}^n\|^2+\|\boldsymbol{u}^{n+1}-\boldsymbol{u}^n\|^2_{C_1\mathbb{M}-\frac{\mathbb{A}}{2}}+\frac{1}{2}\left(\|\boldsymbol{u}^{n+1}\|^2_{\mathbb{A}}-\|\boldsymbol{u}^n\|^2_{\mathbb{A}}\right)\le\frac{1}{\Delta t}\|\boldsymbol{u}^{n+1}-\boldsymbol{u}^n\|^2+\frac{\Delta t}{4}\|\boldsymbol{f}^n\|^2 \tag{31}$$

By assumption, $C_1\mathbb{M}-\frac{\mathbb{A}}{2}\ge 0$, therefore

$$\frac{1}{2}\left(\|\boldsymbol{u}^{n+1}\|^2_{\mathbb{A}}-\|\boldsymbol{u}^n\|^2_{\mathbb{A}}\right)\le\frac{\Delta t}{4}\|\boldsymbol{f}^n\|^2 \tag{32}$$

which leads to (24) after summing over n.

The energy norm estimate (24) along is sufficient to assert unconditional stability of (23). For sake of completeness, we proceed with the L^2 estimate (25). Take the standard inner product with $\boldsymbol{u}^{n+1}+\boldsymbol{u}^n$ on both sides of (27) to get

$$\|\boldsymbol{u}^{n+1}\|^2_{\mathbb{Q}}-\|\boldsymbol{u}^n\|^2_{\mathbb{Q}}+\frac{1}{2}\|\boldsymbol{u}^{n+1}+\boldsymbol{u}^n\|^2_{\mathbb{A}}-\frac{1}{2}\Big(\|\boldsymbol{u}^{n+1}\|^2_{\mathbb{A}}-\|\boldsymbol{u}^{n+1}\|^2_{\mathbb{A}}\Big)=\langle\boldsymbol{u}^{n+1}+\boldsymbol{u}^n,\boldsymbol{f}^n\rangle \tag{33}$$

it follows that

$$\|\boldsymbol{u}^{n+1}\|^2_{\mathbb{Q}-\frac{\mathbb{A}}{2}}-\|\boldsymbol{u}^n\|^2_{\mathbb{Q}-\frac{\mathbb{A}}{2}}+\frac{1}{2}\|\boldsymbol{u}^{n+1}+\boldsymbol{u}^n\|^2_{\mathbb{A}}\le\frac{1}{2}\|\boldsymbol{u}^{n+1}+\boldsymbol{u}^n\|^2_{\mathbb{A}}+\frac{1}{2}\|\boldsymbol{f}^n\|^2_{\mathbb{A}^{-1}} \tag{34}$$

From (34) and (30), we have

$$\Big(\|\boldsymbol{u}^{n+1}\|^2+\Delta t\|\boldsymbol{u}^{n+1}\|^2_{C_1\mathbb{M}-\frac{\mathbb{A}}{2}}\Big)-\Big(\|\boldsymbol{u}^n\|^2+\Delta t\|\boldsymbol{u}^n\|^2_{C_1\mathbb{M}-\frac{\mathbb{A}}{2}}\Big)\le\frac{\Delta t}{2}\|\boldsymbol{f}^n\|^2_{\mathbb{A}^{-1}} \tag{35}$$

which leads directly to (25) upon summing over n. This completes the proof of (25)

□

4.3.2 Stabilized Predictor-Corrector Scheme

In this section, we will give a rigorous stability estimate of the stabilized predictor-corrector scheme:

$$\begin{cases}\dfrac{\boldsymbol{u}^{n+\frac{1}{2}}-\boldsymbol{u}^n}{\frac{\Delta t}{2}}+C_2\mathbb{M}\boldsymbol{u}^{n+\frac{1}{2}}=(C_2\mathbb{M}-\mathbb{A})\boldsymbol{u}^n+\boldsymbol{f}^n\\[2mm]\dfrac{\boldsymbol{u}^{n+1}-\boldsymbol{u}^n}{\Delta t}+C_2\mathbb{M}\dfrac{\boldsymbol{u}^{n+1}+\boldsymbol{u}^n}{2}=(C_2\mathbb{M}-\mathbb{A})\boldsymbol{u}^{n+\frac{1}{2}}+\boldsymbol{f}^{n+\frac{1}{2}}\end{cases} \tag{36}$$

where $\mathbb{M}$ and $\mathbb{A}$ are as in section 4.3.1. Here $C_2\mathbb{M}$ is the matrix representation of the stabilizing term $\mathcal{L}_0$ and C_2 is another undetermined constant.

The discrete energy estimate for the stabilized Backward Euler method (23) in section 4.3.1 can probably be extended to higher order schemes including CN-AB2 as in [37] and BD2/EP2, BD3/EP3 as in [44]. See also [29] for energy estimate of up to BDF5 scheme for Stokes equations. The authors in [38] took a different approach and obtained L^2 error estimate of (13) applied to the isotropic Cahn-Hilliard equation.

Our goal is to establish similar estimates as in Theorem 1 for the second order scheme (36). To this end, we first eliminate the intermediate variable $\boldsymbol{u}^{n+\frac{1}{2}}$ by rewriting the first equation of (36) as

$$\Big(\frac{2}{\Delta t}+C_2\mathbb{M}\Big)\boldsymbol{u}^{n+\frac{1}{2}}=\Big(\frac{2}{\Delta t}+C_2\mathbb{M}-\mathbb{A}\Big)\boldsymbol{u}^{n}+\boldsymbol{f}^{n} \tag{37}$$

and substitute it back to get

$$\begin{aligned}\Big(\frac{1}{\Delta t}+\frac{C_2\mathbb{M}}{2}\Big)\boldsymbol{u}^{n+1}= &\Big(\frac{1}{\Delta t}+\frac{C_2\mathbb{M}}{2}-\mathbb{A}-(C_2\mathbb{M}-\mathbb{A})\big(\frac{2}{\Delta t}+C_2\mathbb{M}\big)^{-1}\mathbb{A}\Big)\boldsymbol{u}^{n}\\ &+(C_2\mathbb{M}-\mathbb{A})\big(\frac{2}{\Delta t}+C_2\mathbb{M}\big)^{-1}\boldsymbol{f}^{n}+\boldsymbol{f}^{n+\frac{1}{2}}\end{aligned} \tag{38}$$

To simplify the expression, we denote by

$$\mathbb{Q}_2\equiv\Big(\frac{2}{\Delta t}+C_2\mathbb{M}\Big)=\mathbb{Q}_2^{\mathrm{T}}>0, \tag{39}$$

$$\mathbb{T}\equiv(C_2\mathbb{M}-\mathbb{A})=\mathbb{T}^{\mathrm{T}}>0, \tag{40}$$

and rewrite (38) as

$$\begin{aligned}\tfrac{1}{2}\mathbb{Q}_2\boldsymbol{u}^{n+1} &=\big(\tfrac{1}{2}\mathbb{Q}_2-\mathbb{A}-\mathbb{T}\mathbb{Q}_2^{-1}\mathbb{A}\big)\,\boldsymbol{u}^{n}+\mathbb{T}\mathbb{Q}_2^{-1}\boldsymbol{f}^{n}+\boldsymbol{f}^{n+\frac{1}{2}}\\ &=\big(\tfrac{1}{2}\mathbb{Q}_2-\big(\mathbb{I}+\mathbb{T}\mathbb{Q}_2^{-1}\big)\mathbb{A}\big)\,\boldsymbol{u}^{n}+\mathbb{T}\mathbb{Q}_2^{-1}\boldsymbol{f}^{n}+\boldsymbol{f}^{n+\frac{1}{2}}\\ &=\big(\tfrac{1}{2}\mathbb{Q}_2-\big(\mathbb{Q}_2+\mathbb{T}\big)\mathbb{Q}_2^{-1}\mathbb{A}\big)\,\boldsymbol{u}^{n}+\mathbb{T}\mathbb{Q}_2^{-1}\boldsymbol{f}^{n}+\boldsymbol{f}^{n+\frac{1}{2}}\end{aligned} \tag{41}$$

or

$$\boldsymbol{u}^{n+1}=(\mathbb{I}-2\mathbb{Q}_2^{-1}\big(\mathbb{Q}_2+\mathbb{T}\big)\mathbb{Q}_2^{-1}\mathbb{A})\boldsymbol{u}^{n}+2\mathbb{Q}_2^{-1}\mathbb{T}\mathbb{Q}_2^{-1}\boldsymbol{f}^{n}+2\mathbb{Q}_2^{-1}\boldsymbol{f}^{n+\frac{1}{2}}=(\mathbb{I}-\mathbb{S}^{-1}\mathbb{A})\boldsymbol{u}^{n}+\boldsymbol{g}^{n} \tag{42}$$

where

$$\mathbb{S}\equiv\frac{1}{2}\mathbb{Q}_2(\mathbb{Q}_2+\mathbb{T})^{-1}\mathbb{Q}_2 \tag{43}$$

and

$$\boldsymbol{g}^{n}\equiv2\mathbb{Q}_2^{-1}\mathbb{T}\mathbb{Q}_2^{-1}\boldsymbol{f}^{n}+2\mathbb{Q}_2^{-1}\boldsymbol{f}^{n+\frac{1}{2}}. \tag{44}$$

It is crucial to note that

$$\mathbb{S}=\mathbb{S}^{\mathrm{T}}>0, \tag{45}$$

therefore (36) can be symmetrized and put in a form that completely resembles the 1st order scheme (27):

$$\mathbb{S}(\boldsymbol{u}^{n+1}-\boldsymbol{u}^{n})+\mathbb{A}\boldsymbol{u}^{n}=\mathbb{S}\boldsymbol{g}^{n} \tag{46}$$

Upon comparing (27) with (42), and inspecting the left hand side of (29) and (34), it is clear that the following estimates are crucial for the estimates of the 2nd order scheme (46):

Lemma 1. *If* $\mathbb{A} = \mathbb{A}^{\mathrm{T}} > 0$, $\mathbb{M} = \mathbb{M}^{\mathrm{T}} > 0$ *and* $C_2\mathbb{M} \geq \mathbb{A}$, *then*

(i)

$$\frac{\mathbb{A}}{2} + \frac{1}{\Delta t} \leq \mathbb{S} \tag{47}$$

(ii)

$$\frac{\mathbb{Q}_2}{4} \leq \mathbb{S} \leq \frac{\mathbb{Q}_2}{2}. \tag{48}$$

where $\mathbb{S}$, $\mathbb{Q}_2$ *are defined by* (43), (39) *and* (40).

Proof. **Part (i)**: Denote by $\mathbb{B} = \mathbb{A} + \dfrac{2}{\Delta t}$, and $\lambda_{\max}$, $\mu_{\max}$ the maximal eigenvalue of

$$\mathbb{B}\boldsymbol{v} = \lambda\mathbb{Q}_2\boldsymbol{v}, \qquad \text{and} \qquad \mathbb{B}\boldsymbol{v} = \mu\mathbb{S}\boldsymbol{v}, \tag{49}$$

respectively, where $\mathbb{Q}_2$ is given by (26). We will show that

$$\mathbb{A} \leq C_2\mathbb{M} \implies \lambda_{\max} \leq 1 \implies \mu_{\max} \leq 2 \tag{50}$$

The first implication is obvious since $\lambda_{\max} \leq 1$ if and only if $\mathbb{B} \leq \mathbb{Q}_2$. As to the second implication, we first note that the pencils in (49) are isospectral to

$$\mathbb{B}^{\frac{1}{2}}\mathbb{Q}^{-1}\mathbb{B}^{\frac{1}{2}}\boldsymbol{w} = \lambda\boldsymbol{w} \qquad \text{and} \qquad \mathbb{B}^{\frac{1}{2}}\mathbb{S}^{-1}\mathbb{B}^{\frac{1}{2}}\boldsymbol{w} = \mu\boldsymbol{w}, \tag{51}$$

respectively (where $\boldsymbol{w} = \mathbb{B}^{\frac{1}{2}}\boldsymbol{v}$). Therefore

$$\begin{aligned}
\mu_{\max} &\leq \max_{\boldsymbol{x}\in\mathbf{R}^{M-1}\setminus\{\mathbf{0}\}} 2\,\frac{\boldsymbol{x}^{\mathrm{T}}\mathbb{B}^{\frac{1}{2}}\mathbb{S}^{-1}\mathbb{B}^{\frac{1}{2}}\boldsymbol{x}}{\boldsymbol{x}^{\mathrm{T}}\boldsymbol{x}} \\
&= \max_{\boldsymbol{x}\in\mathbf{R}^{M-1}\setminus\{\mathbf{0}\}} 2\,\frac{\boldsymbol{x}^{\mathrm{T}}\mathbb{B}^{\frac{1}{2}}\mathbb{Q}_2{}^{-1}(2\mathbb{Q}_2 - \mathbb{B})\mathbb{Q}_2{}^{-1}\mathbb{B}^{\frac{1}{2}}\boldsymbol{x}}{\boldsymbol{x}^{\mathrm{T}}\boldsymbol{x}} \qquad (\text{since } \mathbb{Q}_2 + \mathbb{T} = 2\mathbb{Q}_2 - \mathbb{B}) \\
&= \max_{\boldsymbol{x}\in\mathbf{R}^{M-1}\setminus\{\mathbf{0}\}} 2\,\frac{\boldsymbol{x}^{\mathrm{T}}\left(\mathbb{B}^{\frac{1}{2}}\mathbb{Q}_2{}^{-1}\mathbb{B}^{\frac{1}{2}}\right)\left(\mathbb{B}^{-\frac{1}{2}}(2\mathbb{Q}_2 - \mathbb{B})\mathbb{B}^{-\frac{1}{2}}\right)\left(\mathbb{B}^{\frac{1}{2}}\mathbb{Q}_2{}^{-1}\mathbb{B}^{\frac{1}{2}}\right)\boldsymbol{x}}{\boldsymbol{x}^{\mathrm{T}}\boldsymbol{x}} \\
&= \max_{\boldsymbol{x}\in\mathbf{R}^{M-1}\setminus\{\mathbf{0}\}} 2\,\frac{\boldsymbol{x}^{\mathrm{T}}\widehat{\mathbb{B}}(2\widehat{\mathbb{B}}^{-1} - 1)\widehat{\mathbb{B}}\boldsymbol{x}}{\boldsymbol{x}^{\mathrm{T}}\boldsymbol{x}}, \qquad \text{where} \quad \widehat{\mathbb{B}} \equiv \mathbb{B}^{\frac{1}{2}}\mathbb{Q}_2{}^{-1}\mathbb{B}^{\frac{1}{2}}
\end{aligned} \tag{52}$$

From (51) and the definition of $\widehat{\mathbb{B}}$, we see that

$$\mu_{\max} \leq 2\max_j \lambda_j\Big(2\frac{1}{\lambda_j} - 1\Big)\lambda_j = \max_j\left(4\lambda_j - 2\lambda_j^2\right) = \max_j 2\Big(1 - \left(1 - \lambda_j\right)^2\Big) \tag{53}$$

Since $\lambda_j \leq \lambda_{\max} \leq 1$, it follows that $\mu_{\max} \leq 2$. This completes the proof of (50), hence (47).

Part (ii): Since

$$\mathbb{S} = \frac{1}{2}\mathbb{Q}_2(\mathbb{Q}_2 + \mathbb{T})^{-1}\mathbb{Q}_2 = \mathbb{Q}_2(\frac{4}{\Delta t} + 4C_2\mathbb{M} - 2\mathbb{A})^{-1}\mathbb{Q}_2 \tag{54}$$

Therefore, since $C_2\mathbb{M} > \mathbb{A}$,

$$\frac{4}{\Delta t} + 4C_2\mathbb{M} - 2\mathbb{A} \geq \frac{4}{\Delta t} + 2C_2\mathbb{M} = 2\mathbb{Q}_2. \tag{55}$$

On the other hand

$$\frac{4}{\Delta t} + 4C_2\mathbb{M} - 2\mathbb{A} \leq \frac{4}{\Delta t} + 4C_2\mathbb{M} \leq 4\mathbb{Q}_2 \tag{56}$$

thus (48) follows from (54), (55), and (56). □

Theorem 2. *Under the same assumptions in Lemma 1, the stabilized predictor-corrector scheme (36) (or (46)) is unconditionally stable and admits the following estimates:*

$$\|\boldsymbol{u}^N\|^2_{\mathbb{A}} \leq \|\boldsymbol{u}^0\|^2_{\mathbb{A}} + \Delta t \sum_{n=0}^{N-1} \left(\|\boldsymbol{f}^n\|^2 + \|\boldsymbol{f}^{n+\frac{1}{2}}\|^2\right) \tag{57}$$

and

$$\|\boldsymbol{u}^N\|^2 \leq \|\boldsymbol{u}^0\|^2 + \frac{\Delta t}{2}C_2\|\boldsymbol{u}^0\|^2_{\mathbb{M}} + \Delta t \sum_{n=0}^{N-1} \left(\|\boldsymbol{f}^n\|^2_{\mathbb{A}^{-1}} + \|\boldsymbol{f}^{n+\frac{1}{2}}\|^2_{\mathbb{A}^{-1}}\right) \tag{58}$$

Proof. **Proof of** (57):

Similar to the derivation of (29), we can obtain the following estimate from (46):

$$\|\boldsymbol{u}^{n+1} - \boldsymbol{u}^n\|^2_{\mathbb{S}-\frac{\mathbb{A}}{2}} + \frac{1}{2}(\|\boldsymbol{u}^{n+1}\|^2_{\mathbb{A}} - \|\boldsymbol{u}^n\|^2_{\mathbb{A}}) = \langle \boldsymbol{u}^{n+1} - \boldsymbol{u}^n, \mathbb{S}\boldsymbol{g}^n \rangle \tag{59}$$

With (47) and the inequality

$$\langle \boldsymbol{u}^{n+1} - \boldsymbol{u}^n, \mathbb{S}\boldsymbol{g}^n \rangle \leq \frac{1}{\Delta t}\|\boldsymbol{u}^{n+1} - \boldsymbol{u}^n\|^2 + \frac{\Delta t}{4}\|\mathbb{S}\boldsymbol{g}^n\|^2, \tag{60}$$

we see that

$$\frac{1}{2}(\|\boldsymbol{u}^{n+1}\|^2_{\mathbb{A}} - \|\boldsymbol{u}^n\|^2_{\mathbb{A}}) \leq \frac{\Delta t}{4}\|\mathbb{S}\boldsymbol{g}^n\|^2. \tag{61}$$

To estimate the right hand side of (61), we note from (44) that

$$\|\mathbb{S}\boldsymbol{g}^n\|^2 \leq 2\|2\mathbb{S}\mathbb{Q}_2^{-1}\mathbb{T}\mathbb{Q}_2^{-1}\boldsymbol{f}^n\|^2 + 2\|2\mathbb{S}\mathbb{Q}_2^{-1}\boldsymbol{f}^{n+\frac{1}{2}}\|^2 \tag{62}$$

It suffices to estimate $\mathbb{Q}_2^{-1}\mathbb{T}\mathbb{Q}_2^{-1}\mathbb{S}^2\mathbb{Q}_2^{-1}\mathbb{T}\mathbb{Q}_2^{-1}$ and $\mathbb{Q}_2^{-1}\mathbb{S}^2\mathbb{Q}_2^{-1}$.

Since $\mathbb{S} \leq \dfrac{\mathbb{Q}_2}{2}$, and $\mathbb{T} = C_2\mathbb{M} - \mathbb{A} \leq \mathbb{Q}_2$, we have

$$\mathbb{Q}_2^{-1}\mathbb{T}\mathbb{Q}_2^{-1}\mathbb{S}^2\mathbb{Q}_2^{-1}\mathbb{T}\mathbb{Q}_2^{-1} \leq \frac{1}{4}\mathbb{Q}_2^{-1}\mathbb{T}^2\mathbb{Q}_2^{-1} \leq \frac{1}{4}\mathbb{I} \tag{63}$$

and

$$\mathbb{Q}_2^{-1}\mathbb{S}^2\mathbb{Q}_2^{-1} \le \frac{1}{4}\mathbb{I} \tag{64}$$

thus

$$\|\mathbb{S}\boldsymbol{g}^n\|^2 \le 2\|\boldsymbol{f}^n\|^2 + 2\|\boldsymbol{f}^{n+\frac{1}{2}}\|^2. \tag{65}$$

From (61) (65), we obtain

$$\|\boldsymbol{u}^{n+1}\|_{\mathbb{A}}^2 \le \|\boldsymbol{u}^n\|_{\mathbb{A}}^2 + \Delta t\big(\|\boldsymbol{f}^n\|^2 + \|\boldsymbol{f}^{n+\frac{1}{2}}\|^2\big) \tag{66}$$

which completes the proof of (57) after summing over n.

The energy norm estimate (57) along is sufficient for unconditional stability of (36). We proceed with the L^2 estimate (58) for sake of completeness.

Proof of (58):

Recall the derivation that leads to (34) and apply it to (46), we get the analogue of (34) for (46):

$$\|\boldsymbol{u}^{n+1}\|_{\mathbb{S}-\frac{\mathbb{A}}{2}}^2 - \|\boldsymbol{u}^n\|_{\mathbb{S}-\frac{\mathbb{A}}{2}}^2 \le \frac{1}{2}\|\mathbb{S}\boldsymbol{g}^n\|_{\mathbb{A}^{-1}}^2 \tag{67}$$

It remains to estimate $\|\mathbb{S}\boldsymbol{g}^n\|_{\mathbb{A}^{-1}}^2$. From (44), we have

$$\begin{aligned}\mathbb{S}\boldsymbol{g}^n &= \mathbb{Q}_2(\mathbb{Q}_2+\mathbb{T})^{-1}\mathbb{Q}_2(\mathbb{Q}_2^{-1}\mathbb{T}\mathbb{Q}_2^{-1}\boldsymbol{f}^n + \mathbb{Q}_2^{-1}\boldsymbol{f}^{n+\frac{1}{2}})\\ &= (\mathbb{Q}_2^{-1} + \mathbb{Q}_2^{-1}\mathbb{T}\mathbb{Q}_2^{-1})^{-1}(\mathbb{Q}_2^{-1}\mathbb{T}\mathbb{Q}_2^{-1}\boldsymbol{f}^n + \mathbb{Q}_2^{-1}\boldsymbol{f}^{n+\frac{1}{2}})\end{aligned} \tag{68}$$

Consequently,

$$\begin{aligned}\|\mathbb{S}\boldsymbol{g}^n\|_{\mathbb{A}^{-1}}^2 \le{}& 2\|(\mathbb{Q}_2^{-1} + \mathbb{Q}_2^{-1}\mathbb{T}\mathbb{Q}_2^{-1})^{-1}\mathbb{Q}_2^{-1}\mathbb{T}\mathbb{Q}_2^{-1}\boldsymbol{f}^n\|_{\mathbb{A}^{-1}}^2\\ &+ 2\|(\mathbb{Q}_2^{-1} + \mathbb{Q}_2^{-1}\mathbb{T}\mathbb{Q}_2^{-1})^{-1}\mathbb{Q}_2^{-1}\boldsymbol{f}^{n+\frac{1}{2}}\|_{\mathbb{A}^{-1}}^2\end{aligned} \tag{69}$$

The first term on the right hand side of (69) can be estimated by

$$\begin{aligned}&\|(\mathbb{Q}_2^{-1} + \mathbb{Q}_2^{-1}\mathbb{T}\mathbb{Q}_2^{-1})^{-1}\mathbb{Q}_2^{-1}\mathbb{T}\mathbb{Q}_2^{-1}\boldsymbol{f}^n\|_{\mathbb{A}^{-1}}^2\\ =&\|\mathbb{A}^{-\frac{1}{2}}(\mathbb{Q}_2^{-1} + \mathbb{Q}_2^{-1}\mathbb{T}\mathbb{Q}_2^{-1})^{-1}\mathbb{Q}_2^{-1}\mathbb{T}\mathbb{Q}_2^{-1}\boldsymbol{f}^n\|^2\\ =&\|(\mathbb{A}^{\frac{1}{2}}\mathbb{Q}_2^{-1}\mathbb{A}^{\frac{1}{2}} + \mathbb{A}^{\frac{1}{2}}\mathbb{Q}_2^{-1}\mathbb{T}\mathbb{Q}_2^{-1}\mathbb{A}^{\frac{1}{2}})^{-1}(\mathbb{A}^{\frac{1}{2}}\mathbb{Q}_2^{-1}\mathbb{T}\mathbb{Q}_2^{-1}\mathbb{A}^{\frac{1}{2}})\mathbb{A}^{-\frac{1}{2}}\boldsymbol{f}^n\|^2\\ \le&\|\mathbb{A}^{-\frac{1}{2}}\boldsymbol{f}^n\|^2 = \|\boldsymbol{f}^n\|_{\mathbb{A}^{-1}}^2\end{aligned} \tag{70}$$

where we have used the fact that if $\mathbb{P} = \mathbb{P}^{\mathrm{T}} > 0$, $\mathbb{Q} = \mathbb{Q}^{\mathrm{T}} > 0$, then $\mathbb{P}(\mathbb{P}+\mathbb{Q})^{-2}\mathbb{P} < \mathbb{P}(\mathbb{P})^{-2}\mathbb{P} = \mathbb{I}$. Similarly, the second term is bounded by

$$\|(\mathbb{Q}_2^{-1} + \mathbb{Q}_2^{-1}\mathbb{T}\mathbb{Q}_2^{-1})^{-1}\mathbb{Q}_2^{-1}\boldsymbol{f}^{n+\frac{1}{2}}\|_{\mathbb{A}^{-1}}^2 \le \|\boldsymbol{f}^{n+\frac{1}{2}}\|_{\mathbb{A}^{-1}}^2 \tag{71}$$

thus

$$\|\mathbb{S}\boldsymbol{g}^n\|_{\mathbb{A}^{-1}}^2 \le 2\|\boldsymbol{f}^n\|_{\mathbb{A}^{-1}}^2 + 2\|\boldsymbol{f}^{n+\frac{1}{2}}\|_{\mathbb{A}^{-1}}^2. \tag{72}$$

After summing (67) over n and applying the estimate (72), we get

$$\|\boldsymbol{u}^N\|^2_{\mathbb{S}-\frac{\mathbb{A}}{2}} \leq \|\boldsymbol{u}^0\|^2_{\mathbb{S}-\frac{\mathbb{A}}{2}} + \sum_{n=0}^{N-1} \left(\|\boldsymbol{f}^n\|^2_{\mathbb{A}^{-1}} + \|\boldsymbol{f}^{n+\frac{1}{2}}\|^2_{\mathbb{A}^{-1}}\right) \tag{73}$$

From (47) and (48) and (72), we have

$$\frac{1}{\Delta t}\|\boldsymbol{u}^N\|^2 \leq \frac{1}{2}\left(C_2\|\boldsymbol{u}^0\|^2_{\mathbb{M}} + \frac{2}{\Delta t}\|\boldsymbol{u}^0\|^2\right) + \sum_{n=0}^{N-1} \left(\|\boldsymbol{f}^n\|^2_{\mathbb{A}^{-1}} + \|\boldsymbol{f}^{n+\frac{1}{2}}\|^2_{\mathbb{A}^{-1}}\right) \tag{74}$$

Thus (58) follows from multiplying (74) by Δt. □